

FIG. 3. Dephosphorylation reverses the molecular mass shift of N-terminal parkin both in HEK293 cells and SH-SY5Y cells. *A*, schematic representation of MYC-parkin-V5, MYC-parN-V5, MYC-parNM-V5, and MYC-parC-V5. *B*, the indicated constructs were transiently transfected into HEK293 cells (*left panels*) and SH-SY5Y cells (*right panels*). Twenty-four h after the transfection, 1 μ M OA (*lanes 2, 3, 5, 6, 8, 9, 11, and 12*) or Me₂SO (*lanes 1, 4, 7, and 10*) was added and cultured for 2 h. Immunoprecipitation (IP) was carried out using MYC-agarose beads. Immunoprecipitates were incubated in the presence (*lanes 3, 6, 9, and 12*) or absence (*lanes 1, 2, 4, 5, 7, 8, 10, and 11*) of CIP. Samples were subjected to 10–20% Tris-glycine gel (Invitrogen) or 15% SDS-PAGE. *, unspecific band. The band shifts of full-length parkin from SH-SY5Y cells are better seen on a short exposure (*inset*). *C*, parkin expression levels in each transient transfectant treated with Me₂SO (*lanes 1, 3, 5, and 7*) or OA (*lanes 2, 4, 6, and 8*) were confirmed by immunoblotting (IB) of cell lysates using anti-V5 antibody (*lower panels*).

phoresis, and immunoblots were probed with anti-V5 antibody. MYC-parN-V5 immunoprecipitated from OA-treated cells showed retarded electrophoretic mobility compared with controls (Fig. 3*B*). Full-length MYC-parkin-V5 also showed slight band retardation after OA treatment. These phosphorylation-induced band shifts were observed both in HEK293 and SH-SY5Y cells, indicating similar phosphorylation patterns in non-neuronal neuronal cells. The phosphorylation-induced band retardations were reversed upon CIP treatment (Fig. 3*B*), con-

firmed that phosphorylation in the N terminus of parkin occurs along with a characteristic band shift. Electrophoretic mobility shift caused by the incorporation of covalent phosphate is frequently observed in phosphorylated proteins (*e.g.* tau (32) and the C-terminal fragment of presenilin-1 (33)). On the other hand, band shifts were hardly observed in parNM and parC, despite the fact that parC was phosphorylated *in vivo* (Fig. 2). Note that a band shift is not always a consequence of phosphorylation (34).

Identification of Parkin Phosphorylation Sites—To identify the phosphorylated residues of parkin in OA-treated cells, phosphoamino acid analysis was carried out. Stable transfectants of MYC-parkin in HEK293 cells and SH-SY5Y cells as well as MYC-parN and MYC-parC in HEK293 cells were labeled with [32 P]orthophosphate in the presence of OA. Myc immunoprecipitates were subjected to SDS-PAGE and then transferred onto PVDF. Proteins were eluted from the excised bands and hydrolyzed. Phosphoamino acid analysis revealed that parkin was mainly phosphorylated at serine residues in OA-treated HEK293 cells and SH-SY5Y cells (Fig. 4). Some minor threonine phosphorylation was observed, whereas tyrosine phosphorylation was not evident under these conditions.

There are 30 serine residues in parkin, 14 of them in parN and 4 in parC. We carried out site-directed mutagenesis to identify phosphorylated serine sites. Selected serines with high phosphorylation probability identified with the NetPhos 2.0 prediction algorithm were substituted by alanine in order to generate unphosphorylatable forms. Since there are only 4 serines in parC (Ser²⁹⁶, Ser³⁷⁸, Ser³⁸⁴, and Ser⁴⁰⁷), we mutagenized all of them. These serine-to-alanine mutants in parN and parC as well as wild type with Myc tag at the N terminus and V5 tag at the C terminus were transiently transfected into HEK293 cells, and then cells were labeled with [32 P]orthophosphate in the presence or absence of OA. Cell lysates were subjected to immunoprecipitation using Myc-agarose beads. Phosphate incorporation of S101A, S131A, and S136A mutations under the treatment of OA were reduced compared with wild type parN (Fig. 5A). In the case of [S101A]parN, the shifted band was no longer detected. Thus, Ser¹⁰¹ was found to be the responsible phosphate acceptor for the motility shift of parN. 32 PO₄ incorporation into the lower band was detectable but reduced for the S101A, S131A, and S136A mutants of parN. We also carried out mass spectrometry to determine phosphorylation sites in parN and confirmed that Ser¹³¹ and Ser¹³⁶ (Fig. 5, B and C) were unambiguously phosphorylated, with weaker signals for Ser¹³¹ than for Ser¹³⁶. The phosphorylation of Ser¹⁰¹ was not detected by mass spectrometry analysis, since Lys-C proteolysis of parN could not provide complete coverage of the protein sequence.

In the case of parC, S296A was the only mutant that revealed a small but reproducible reduction of phosphate incorporation compared with wild type parC in the presence of OA (Fig. 5D). No difference of phosphate incorporation between wild type parC and mutants S384A and S407A was detected. However, Ser³⁷⁸ was clearly identified as phosphorylation site using an alternative assay (see below). Taken together, we discovered that Ser¹⁰¹, Ser¹³¹, and Ser¹³⁶ in the parkin N terminus as well as Ser²⁹⁶ (Fig. 5) and Ser³⁷⁸ (see Fig. 7B) in the parkin C terminus are phosphorylated.

Parkin Is Phosphorylated by CK-1, PKA, and PKC—*In vitro* phosphorylation assays were carried out in order to identify kinases involved in phosphorylation of parkin. Fusion proteins GST-parkin, GST-parN, and GST-parC as well as mutations GST-[S101A]parN, GST-[S131A]parN, GST-[S136A]parN, GST-[S296A]parC, and GST-[S378A]parC were expressed in *Escherichia coli*. The recombinant parkin fusion proteins were incubated in the presence of [γ - 32 P]ATP with various protein kinases. CK-1, CK-2, PKA, PKC were chosen because several recognition consensus sites for CK-2, PKA, and PKC were predicted by NetPhos 2.0 algorithm. The antiapoptotic kinase Akt/PKB1 was also considered, because parkin has been reported to protect dopaminergic cells against apoptosis (19–22). GST-parkin as well as GST-parN and GST-parC were efficiently phosphorylated by CK-1, PKA, and PKC, but not by CK-2 and Akt/PKB1 (Fig. 6A).

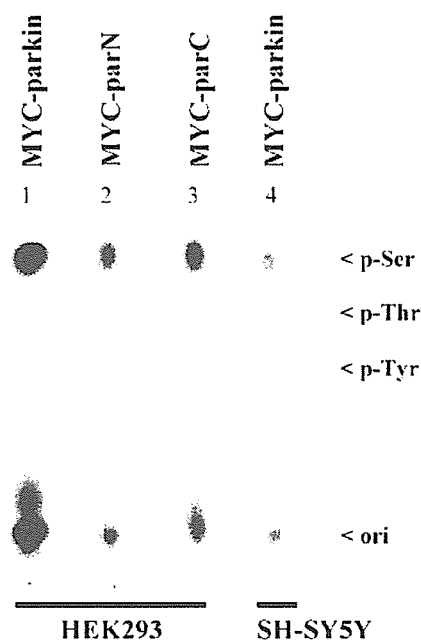


FIG. 4. Parkin is phosphorylated mainly on serine residues. HEK293 cells (lanes 1–3) and SH-SY5Y cells (lane 4) stably expressing the indicated MYC-parkin constructs were used for an *in vivo* phosphorylation assay labeled with [32 P]orthophosphate. Radiolabeled MYC-parkin (lanes 1 and 4), MYC-parN (lane 2), and MYC-parC (lane 3) were isolated by immunoprecipitation and subjected to one-dimensional phosphoamino acid analysis.

We analyzed further which kinases were responsible for selective phosphorylation of residues Ser¹⁰¹, Ser¹³¹, Ser¹³⁶, Ser²⁹⁶, and Ser³⁷⁸. *In vitro* phosphorylation assays were performed using GST fusion proteins harboring serine-to-alanine mutations. Phosphorylation by CK-1 was reduced in GST-[S101A]parN (Fig. 6B) and GST-[S378A]parC (Fig. 6C). We detected slightly reduced phosphorylation of GST-[S101A]parN, GST-[S131A]parN and GST-[S136A]parN by PKA, which indicates that PKA might possibly phosphorylate these serine sites. On the other hand, PKC-mediated phosphate incorporation was not reduced in the serine-to-alanine mutants investigated (Fig. 6, B and C). Thus, PKC was not responsible for phosphorylation of these sites.

We further analyzed whether CK-1, PKA and PKC phosphorylate GST-parN and GST-parC in cell lysates. Fusion proteins were incubated with extracts prepared from HEK293 cells, [γ - 32 P]ATP, and OA in the presence or absence of selective inhibitor of CK-1 (hymenialdisine), an inhibitor of PKA (H-89), and an inhibitor of PKC (GF 109203X). PDBu was used to stimulate PKC activity. Consistent with the result from *in vitro* phosphorylation assays (Fig. 6), we found that GST-parN and GST-parC were phosphorylated by cellular extracts in the absence of inhibitors (Fig. 7, A and B). Both parN and parC phosphorylation was completely inhibited with the CK-1 inhibitor hymenialdisine (Fig. 7, A and B), but not in the presence of the PKA inhibitor H-89. Stimulation of PKC with PDBu enhanced phosphorylation of parN and parC, and this effect was reversed with the PKC inhibitor GF 109203X.

Consistent with the *in vitro* phosphorylation assays (Fig. 6), each of the serine-to-alanine mutants (S101A, S131A, S136A, S296A, and S378A) showed reduced phosphorylation in cell lysates (Fig. 7, A and B). The incorporation of phosphate was completely abolished when GST-[S378]parN was incubated with HEK293 lysates. Phosphate incorporation into the S296A mutant was also reduced in this assay, but to a lesser extent. Taken together, parkin is phosphorylated by CK-1, PKA, and

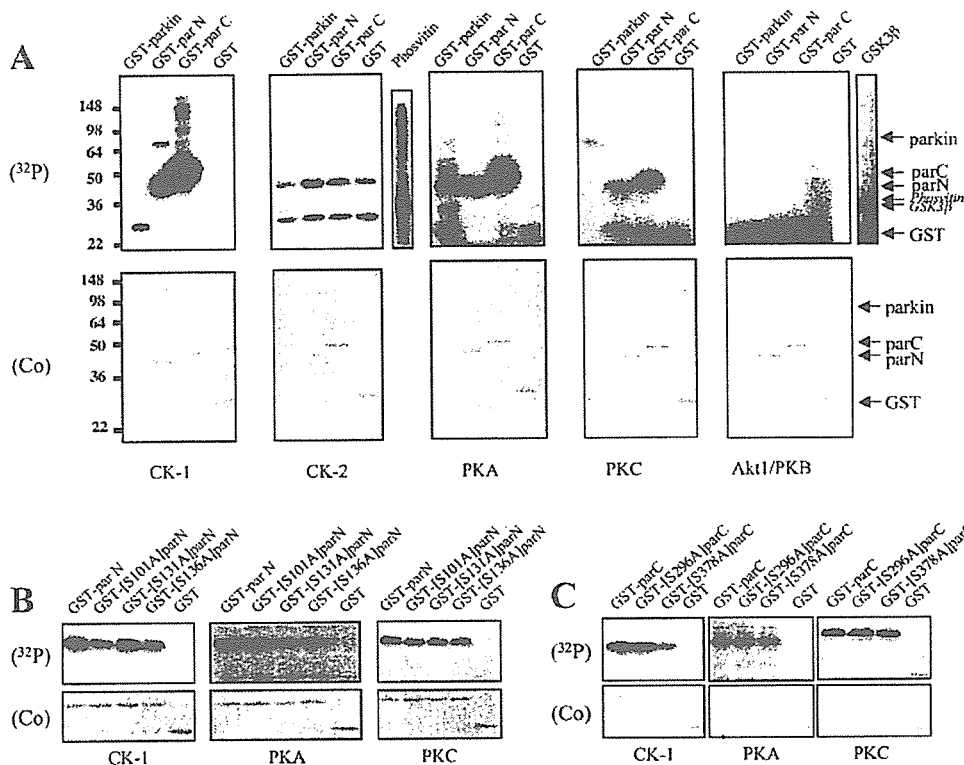


FIG. 6. **CK-1, PKA, and PKC phosphorylate parkin.** A, GST-parkin, GST-parN, and GST-parC were incubated with purified CK-1, CK-2, PKA, PKC, and Akt/PKB1 in the presence of $[\gamma\text{-}^{32}\text{P}]\text{ATP}$. Reaction mixtures were subjected to 12% SDS-PAGE. Phosphorylated fusion proteins were detected by autoradiography (upper panels). Phosvitin, histone, or GSK fusion protein was used as control substrate to confirm activity of CK-1/CK-2, PKA/PKC, or Akt/PKB1, respectively. Equal fusion protein loadings were shown by Coomassie staining (lower panels). B and C, *in vitro* phosphorylation assays were carried out with CK-1 (left panels) PKA (middle panels), and PKC (right panels) using the indicated GST-parN (B) or GST-parC (C) substrates. Experimental procedures were carried out as described in A. Equal substrate protein loading was confirmed by Coomassie staining (lower panels).

anti-FLAG immunoprecipitates were added for reconstitution of an *in vitro* ubiquitination assay. The formation of high molecular weight smears of biotin-ubiquitin in the FLAG immunoprecipitates revealed autoubiquitination of parkin. Overall phosphorylation upon OA treatment of wild-type parkin-transfected cells caused some reduction of parkin autoubiquitination (Fig. 9A).

To provide more quantitative measures of the effect of phosphorylation on parkin activity, we conducted autoubiquitination assays using recombinant GST-parkin phosphorylated *in vitro* with CK-1, PKA, and PKC. Parkin phosphorylation by these kinases reduced parkin activity (Fig. 9B). *In vitro* phosphorylation of GST-parkin decreased its autoubiquitination activity by $24 \pm 8\%$ ($n = 4$) in the case of CK-1, by $44 \pm 5\%$ ($n = 3$) in the case of PKA, and by $39 \pm 12\%$ ($n = 3$) in the case of PKC (Fig. 9C). Thus, phosphorylation of parkin appears to down-regulate its ubiquitin ligase activity.

In the attempt to identify individual regulatory phosphorylation sites within parkin, we investigated FLAG-tagged constructs of the phosphorylation site serine-to-alanine and -aspartate mutants identified above. None of the individual phosphorylation sites investigated appeared to exert a unique regulatory role, as evidenced from densitometric quantification of the autoubiquitinated parkin bands (results not shown). Thus, if parkin E3 activity is regulated by phosphorylation, it must arise from multiple sites.

DISCUSSION

Here we demonstrate that parkin is phosphorylated both in nonneuronal and neuronal cell lines. Parkin appears to be dephosphorylated rapidly under steady state conditions, because the phosphate incorporation was hardly observed with-

out stabilization with OA. At least 5 serine residues were identified as phosphorylation sites. The kinases CK-1, PKA, and PKC were found to phosphorylate parkin. In cells exposed to the Parkinson's disease relevant protein folding stress (38), overall parkin phosphorylation decreased. Unphosphorylated parkin tended to be more active. These findings suggest that phosphorylation of parkin contributes to the regulation of its ubiquitin ligase activity upon unfolded protein stress.

Phosphoamino acid analysis revealed that serine sites are mainly phosphorylated in OA-treated cells. Threonine residues may also be phosphorylated in parkin, because a weak signal was clearly detected. Site-directed mutagenesis combined with *in vivo* and *in vitro* phosphorylation assays led to the identification of Ser¹⁰¹, Ser¹³¹, Ser¹³⁶, Ser²⁹⁶, and Ser³⁷⁸ as phosphorylation sites in parkin. The corresponding serine-to-alanine mutants showed reduced, but not abolished incorporation of phosphate. Thus, multiple phosphorylation sites exist in parkin.

CK-1, PKA, and PKC were identified as putative parkin kinases. Specifically, CK-1 is one kinase to phosphorylate Ser¹⁰¹ and Ser³⁷⁸, because mutations of these sites to alanine strongly reduced incorporation of phosphate. However, the possibility cannot be excluded that other kinases are involved in phosphorylation at these serine sites. CK-1 is an unexpected kinase to phosphorylate parkin because there is no CK-1 recognition consensus sequence ((D/E)XX(S/T)) in the amino acid sequence of parkin. CK-1 is ubiquitously expressed and involved in various important cellular processes, including signal transduction. We also observed a slightly reduced incorporation of phosphate by PKA in S101A, S131A, and S136A, which means that PKA may contribute to phosphorylation of these

FIG. 7. Phosphorylation of N terminus and C terminus by the extracts from HEK293 cells. A and B, cellular extracts from HEK293 cells were incubated with GST-parN (A), GST-parC (B), and various serine-to-alanine mutants plus [γ - 32 P]ATP and 4 μ M OA in the presence or absence of CK-1-selective inhibitor hymenialdisine (5 μ M), PKA-selective inhibitor H-89 (5 μ M), and PKC-selective inhibitor GF 109203X (5 μ M). In order to stimulate PKC, 1 μ M PDBu was added. After the incubation, the precipitation using glutathione-Sepharose was carried out and subjected into 12% SDS-PAGE. Phosphorylated fusion proteins were detected by autoradiography (upper panels). Coomassie stain was carried out to prove the equal protein loading (lower panels). C, the arrows indicate phosphorylation sites in parkin. DMSO, Me₂SO.

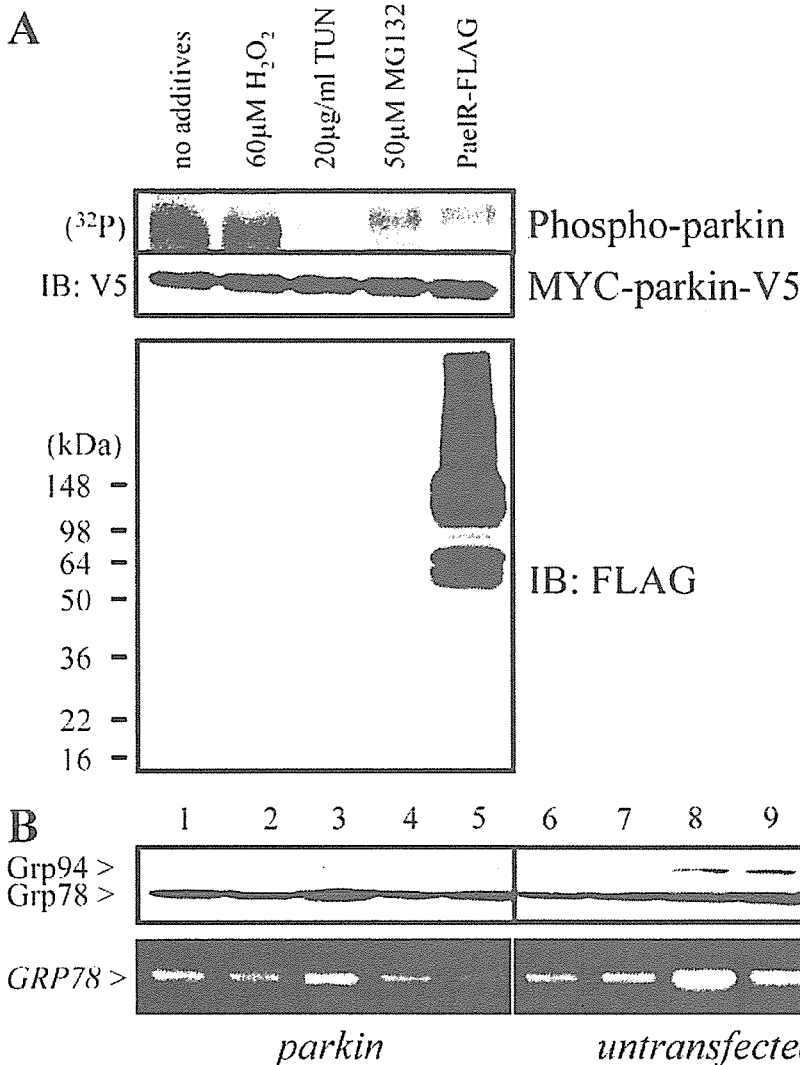
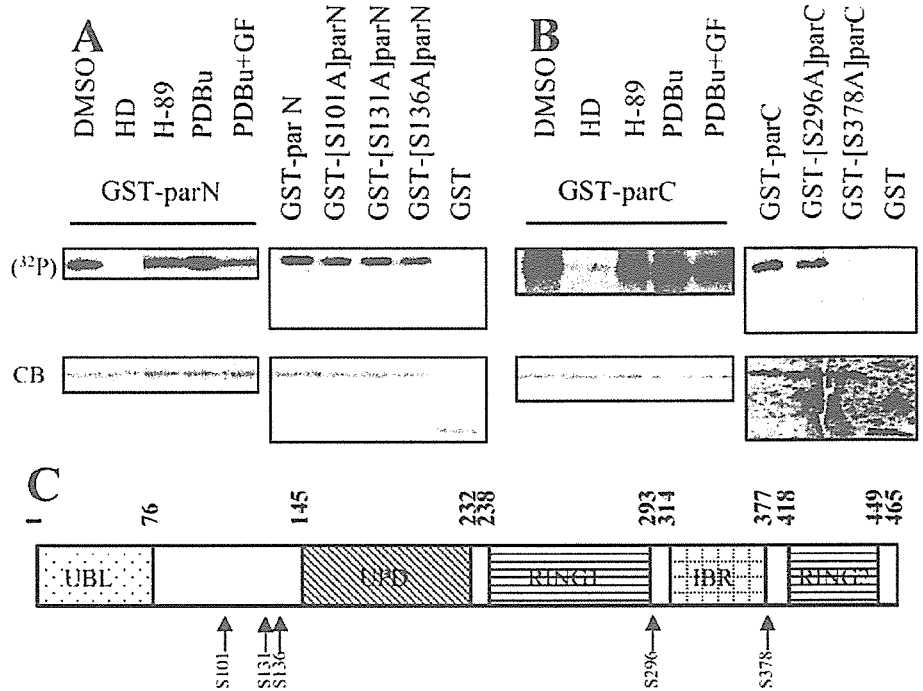
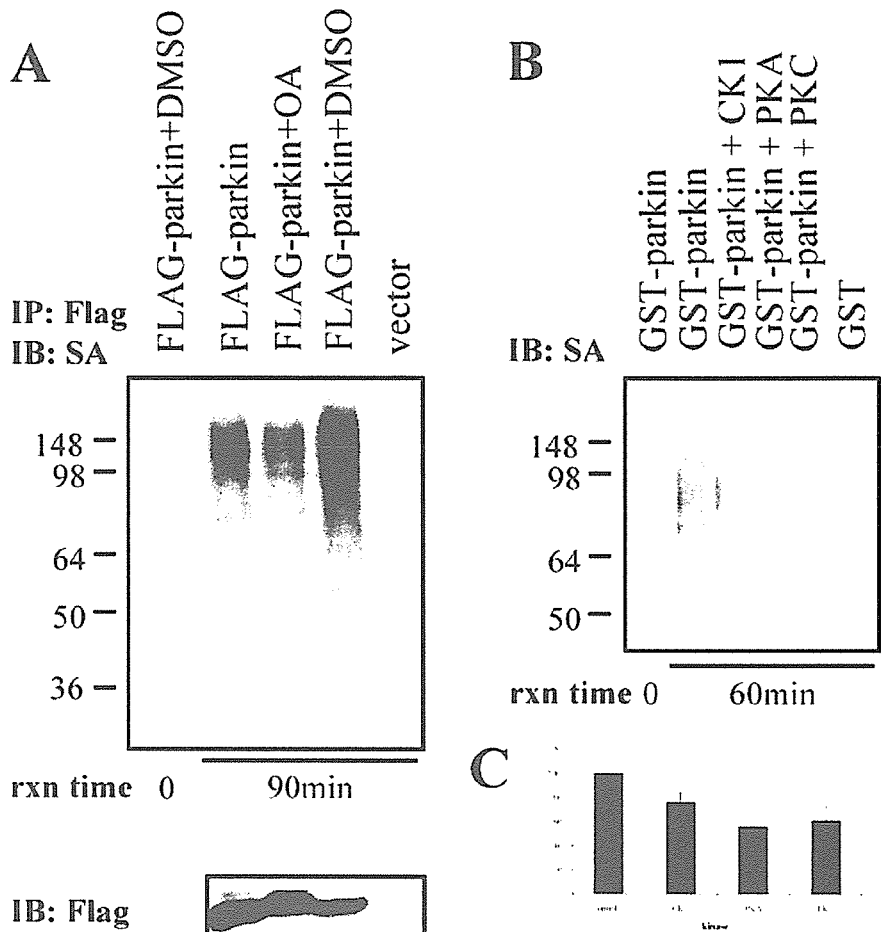


FIG. 8. Phosphorylation of parkin is reduced by ER stress. A, HEK293 cells stably expressing MYC-parkin-V5 were subjected to *in vivo* phosphorylation assay directly (lanes 1–4) or 24 h after transient transfection with PaeIR-FLAG (lane 5). During the 32 P₄ labeling, 1 μ M OA (lanes 1–5) plus no additives (lanes 1 and 5), 60 μ M H₂O₂ (lane 2), 20 μ g/ml tunicamycin (lane 3), or 50 μ M MG132 (lane 4) were administered. Anti-V5 immunoprecipitates were subjected to 12% SDS-PAGE. After electroblotting, phosphorylated proteins were detected by autoradiography (upper panel), and equal expression/loading was confirmed by probing with anti-V5 (middle panel). Overexpression and aggregation of PaeIR-FLAG was confirmed on parallel immunoblots (IB) probed with anti-FLAG (lower panel). B, ER stress was determined by immunoblotting of Grp78 and Grp94 protein (upper panels) and RT-PCR of GRP78 mRNA (lower panels) in HEK293 cells stably transfected with MYC-parkin-V5 (lanes 1–5) or in untransfected HEK293 cells (lanes 6–10). All cells were treated for 3.5 h with 1 μ M OA plus no additives (lanes 1, 5, 6, and 10), 60 μ M H₂O₂ (lanes 2 and 7), 20 μ g/ml tunicamycin (lanes 3 and 8), or 50 μ M MG132 (lanes 4 and 9).

FIG. 9. Phosphorylation down-regulates parkin autoubiquitination activity. A, cellular extracts from transfected HEK293T cells in the presence or absence of OA and Me₂SO were subjected to immunoprecipitation (IP) using FLAG M2-agarose. Immunoprecipitates were incubated with E1, E2 (UbcH7), and biotin-ubiquitin at 30 °C for 90 min reaction (rxn) time (upper panel). Reaction mixtures were subjected to 10% SDS-PAGE and transferred onto PVDF membrane. Ubiquitinated parkin proteins were analyzed by immunoblot (IB) with streptavidin-peroxidase polymer (upper panel). Total lysates were analyzed by immunoblot with anti-FLAG antibody (lower panel). B, GST-parkin immobilized on glutathione-Sepharose was phosphorylated by CK-1, PKA, or PKC. The same experimental procedure was carried out as described in A. C, signal intensities of the streptavidin-binding biotinylated ubiquitin smears generated in experiments performed as described in B were quantified by densitometric scanning and expressed as a percentage of unphosphorylated parkin activity. Error bars, S.E. of four (CK-1) and three (PKA and PKC) experiments, respectively.



sites. PKC is able to phosphorylate parkin but is not responsible for the serine sites investigated here.

Since three identified phosphorylation sites were located in the linker region, and it has been reported that the ubiquitin-like domain interacts with Rpn10, a subunit of 19 S in proteasome (39), we also investigated whether parkin phosphorylation could affect proteasome activities. Each serine-to-alanine or -aspartate mutants still had almost the same level of activities as vector controls (data not shown). The RING-IBR-RING motif of parkin is important to interact with E2 co-enzymes. However, S296A and S378A did not consistently show reduced levels of ubiquitination by *in vitro* ubiquitination assays (data not shown). Although the RING-IBR-RING motif is crucial for parkin ubiquitin ligase function, single site phosphorylation in this domain appears to have no effect on autoubiquitination. Nevertheless, OA-mediated overall phosphorylation of parkin slightly reduced its E3 enzymatic activity. The regulation of parkin E3 activity must be due to multiple phosphorylation sites.

ER stress (but not oxidative stress) was found to specifically reduce parkin phosphorylation levels. Specifically, we found that OA-stabilized phosphorylation of parkin or phosphorylation by identified parkin kinases caused a small but significant reduction of parkin autoubiquitination activity. More *in vivo* work is needed to elucidate if and how parkin phosphorylation affects the activity and recognition of the various substrates of the E3 ubiquitin ligase parkin. In fact, some of the polyubiquitin signals detected in the *in vitro* E3 assay (Fig. 9) may arise from ubiquitination of co-purified, parkin-associated ubiquitin ligase substrates.

Because CK-1 appeared to be a major parkin kinase (Fig. 7), further investigations of signal transduction events involving

CK-1 might be particularly revealing for the regulation of parkin E3 ubiquitin ligase activity. More generally, the involvement of parkin phosphorylation in the ER unfolded protein stress response (Fig. 8) might contribute to the understanding of parkin as dopaminergic neuron survival factor.

Taken together, we suggest that the reduced phosphorylation of parkin in ER stressed cells contributes to the up-regulation of parkin E3 ubiquitin ligase activity, which is believed to suppress cytotoxicity due to unfolded protein stress.

Acknowledgments—We thank J. Walter for technical advice, L. Meijer for providing hymenialdisine, V. Kinzel for the gift of PKA, and V. Lee for the donation of monoclonal anti-parkin. We are grateful to W. Springer, U. Leimer, R. Baumeister, and N. Hattori for parkin constructs.

REFERENCES

- Dauer, W., and Przedborski, S. (2003) *Neuron* **39**, 889–909
- Dawson, T. M., and Dawson, V. L. (2003) *Science* **302**, 819–822
- Kitada, T., Asakawa, S., Hattori, N., Matsumine, H., Yamamura, Y., Minoshima, S., Yokochi, M., Mizuno, Y., and Shimizu, N. (1998) *Nature* **392**, 605–608
- Lücking, C. B., Dürr, A., Bonifati, V., Vaughan, J., De Michele, G., Gasser, T., Harhangi, B. S., Meo, G., Denèfle, P., Wood, N. W., Agid, Y., and Brice, A. (2000) *N. Engl. J. Med.* **342**, 1560–1567
- West, A., Periquet, M., Lincoln, S., Lücking, C. B., Nicholl, D., Bonifati, V., Rawal, N., Gasser, T., Lohmann, E., Deleuze, J.-F., Maraganore, D., Levey, A., Wood, N., Dürr, A., Hardy, J., Brice, A., and Farrer, M. (2002) *Am. J. Med. Genet.* **114**, 584–591
- Kahle, P. J., and Haass, C. (2004) *EMBO Rep.* **5**, 681–685
- Shimura, H., Hattori, N., Kubo, S., Mizuno, Y., Asakawa, S., Minoshima, S., Shimizu, N., Iwai, K., Chiba, T., Tanaka, K., and Suzuki, T. (2000) *Nat. Genet.* **25**, 302–305
- Imai, Y., Soda, M., and Takahashi, R. (2000) *J. Biol. Chem.* **275**, 35661–35664
- Zhang, Y., Gao, J., Chung, K. K. K., Huang, H., Dawson, V. L., and Dawson, T. M. (2000) *Proc. Natl. Acad. Sci. U. S. A.* **97**, 13354–13359
- Cookson, M. R. (2003) *Neuromolecular Med.* **3**, 1–13
- Imai, Y., Soda, M., Inoue, H., Hattori, N., Mizuno, Y., and Takahashi, R. (2001)

Cell **105**, 891–902

12. Chung, K. K. K., Zhang, Y., Lim, K. L., Tanaka, Y., Huang, H., Gao, J., Ross, C. A., Dawson, V. L., and Dawson, T. M. (2001) *Nat. Med.* **7**, 1144–1150
13. Staropoli, J. F., McDermott, C., Martinat, C., Schulman, B., Demireva, E., and Abeliovich, A. (2003) *Neuron* **37**, 735–749
14. Ren, Y., Zhao, J., and Feng, J. (2003) *J. Neurosci.* **23**, 3316–3324
15. Corti, O., Hampe, C., Koutnikova, H., Darios, F., Jacquier, S., Prigent, A., Robinson, J.-C., Pradier, L., Ruberg, M., Mirande, M., Hirsch, E., Rooney, T., Fournier, A., and Brice, A. (2003) *Hum. Mol. Genet.* **12**, 1427–1437
16. Choi, P., Snyder, H., Petrucelli, L., Theisler, C., Chong, M., Zhang, Y., Lim, K., Chung, K. K. K., Kehoe, K., D'Adamio, L., Lee, J. M., Cochran, E., Bowser, R., Dawson, T. M., and Wolozin, B. (2003) *Mol. Brain Res.* **117**, 179–189
17. Huynh, D. P., Scoles, D. R., Nguyen, D., and Pulst, S. M. (2003) *Hum. Mol. Genet.* **12**, 2587–2597
18. Yang, Y., Nishimura, I., Imai, Y., Takahashi, R., and Lu, B. (2003) *Neuron* **37**, 911–924
19. Petrucelli, L., O'Farrell, C., Lockhart, P. J., Baptista, M., Kehoe, K., Vink, L., Choi, P., Wolozin, B., Farrer, M., Hardy, J., and Cookson, M. R. (2002) *Neuron* **36**, 1007–1019
20. Darios, F., Corti, O., Lücking, C. B., Hampe, C., Muriel, M. P., Abbas, N., Gu, W. J., Hirsch, E. C., Rooney, T., Ruberg, M., and Brice, A. (2003) *Hum. Mol. Genet.* **12**, 517–526
21. Higashi, Y., Asanuma, M., Miyazaki, I., Hattori, N., Mizuno, Y., and Ogawa, N. (2004) *J. Neurochem.* **89**, 1490–1497
22. Jiang, H., Ren, Y., Zhao, J., and Feng, J. (2004) *Hum. Mol. Genet.* **13**, 1745–1754
23. Chung, K. K. K., Thomas, B., Li, X., Pletnikova, O., Troncoso, J. C., Marsh, L., Dawson, V. L., and Dawson, T. M. (2004) *Science* **304**, 1328–1331
24. Yao, D., Gu, Z., Nakamura, T., Shi, Z.-Q., Ma, Y., Gaston, B., Palmer, L. A., Rockenstein, E. M., Zhang, Z., Masliah, E., Uehara, T., and Lipton, S. A. (2004) *Proc. Natl. Acad. Sci. U. S. A.* **101**, 10810–10814
25. Pawlyk, A. C., Giasson, B. I., Sampathu, D. M., Perez, F. A., Lim, K. L., Dawson, V. L., Dawson, T. M., Palmiter, R. D., Trojanowski, J. Q., and Lee, V. M.-Y. (2003) *J. Biol. Chem.* **278**, 48120–48128
26. Fountoulakis, M., and Langen, H. (1997) *Anal. Biochem.* **250**, 153–156
27. Wilm, M., and Mann, M. (1996) *Anal. Chem.* **68**, 1–8
28. Jelinek, T., and Weber, M. J. (1993) *BioTechniques* **15**, 628–630
29. Schlossmacher, M. G., Frosch, M. P., Gai, W. P., Medina, M., Sharma, N., Forno, L., Ochiishi, T., Shimura, H., Sharon, R., Hattori, N., Langston, J. W., Mizuno, Y., Hyman, B. T., Selkoe, D. J., and Kosik, K. S. (2002) *Am. J. Pathol.* **160**, 1655–1667
30. Kahns, S., Lykkebo, S., Jakobsen, L. D., Nielsen, M. S., and Jensen, P. H. (2002) *J. Biol. Chem.* **277**, 15303–15308
31. Kahns, S., Kalai, M., Jakobsen, L. D., Clark, B. F. C., Vandenberg, P., and Jensen, P. H. (2003) *J. Biol. Chem.* **278**, 23376–23380
32. Lindwall, G., and Cole, R. D. (1984) *J. Biol. Chem.* **259**, 5301–5305
33. Walter, J., Grünberg, J., Capell, A., Pesold, B., Schindzielorz, A., Citron, M., Mendla, K., St George-Hyslop, P., Multhaup, G., Selkoe, D. J., and Haass, C. (1997) *Proc. Natl. Acad. Sci. U. S. A.* **94**, 5349–5354
34. Okochi, M., Walter, J., Koyama, A., Nakajo, S., Baba, M., Iwatsubo, T., Meijer, L., Kahle, P. J., and Haass, C. (2000) *J. Biol. Chem.* **275**, 390–397
35. Hyun, D.-H., Lee, M., Hattori, N., Kubo, S.-I., Mizuno, Y., Halliwell, B., and Jenner, P. (2002) *J. Biol. Chem.* **277**, 28572–28577
36. Munro, S., and Pelham, H. R. (1986) *Cell* **46**, 291–300
37. Chang, S. C., Erwin, A. E., and Lee, A. S. (1989) *Mol. Cell. Biol.* **9**, 2153–2162
38. Giasson, B. I., and Lee, V. M.-Y. (2001) *Neuron* **31**, 885–888
39. Sakata, E., Yamaguchi, Y., Kurimoto, E., Kikuchi, J., Yokoyama, S., Yamada, S., Kawahara, H., Yokosawa, H., Hattori, N., Mizuno, Y., Tanaka, K., and Kato, K. (2003) *EMBO Rep.* **4**, 301–306

U-box protein carboxyl terminus of Hsc70-interacting protein (CHIP) mediates poly-ubiquitylation preferentially on four-repeat Tau and is involved in neurodegeneration of tauopathy

Shigetsugu Hatakeyama,*† Masaki Matsumoto,*† Takumi Kamura,*† Miyuki Murayama,¶ Du-Hua Chui,¶ Emmanuel Planel,¶ Ryosuke Takahashi,§ Keiichi I. Nakayama*† and Akihiko Takashima¶

*Department of Molecular and Cellular Biology and †Department of Molecular Genetics, Medical Institute of Bioregulation, Fukuoka, Japan

‡CREST, Japan Science and Technology Corporation, Saitama, Japan

§Laboratory for Motor System Neurodegeneration and ¶Laboratory for Alzheimer's Disease, Brain Science Institute, RIKEN, Saitama, Japan

Abstract

Neurofibrillary tangles (NFTs), which are composed of hyperphosphorylated and ubiquitylated tau, are exhibited at regions where neuronal loss occurs in neurodegenerative diseases; however, the mechanisms of NFT formation remain unknown. Molecular studies of frontotemporal dementia with parkinsonism-17 demonstrated that increasing the ratio of tau with exon 10 insertion induced fibrillar tau accumulation. Here, we show that carboxyl terminus of Hsc70-interacting protein (CHIP), a U-box protein, recognizes the microtubule-binding repeat region of tau and preferentially ubiquitylates four-re-

peat tau compared with three-repeat tau. Overexpression of CHIP induced the prompt degradation of tau, reduced the formation of detergent-insoluble tau and inhibited proteasome inhibitor-induced cell death. NFT bearing neurons in progressive supranuclear palsy, in which four-repeat tau is a component, showed the accumulation of CHIP. Thus, CHIP is a ubiquitin ligase for four-repeat tau and maintains neuronal survival by regulating the quality control of tau in neurons.

Keywords: carboxyl terminus of Hsc70-interacting protein, neurodegeneration, neurofibrillary tangle, tau, ubiquitylation. *J. Neurochem.* (2004) **91**, 299–307.

Protein aggregation causes the pathological lesions associated with neurodegenerative disorders (Kopito and Ron 2000). Neurofibrillary tangles (NFTs) emerge when pathological tau protein aggregates accumulate in neurons and form paired helical filament-tau proteins. These aggregates are composed of both ubiquitylated and highly phosphorylated tau and are characteristic of several neurodegenerative diseases, including Alzheimer's disease (Selkoe 2000; Lee *et al.* 2001; Hardy and Selkoe 2002). Of the several kinases that play a role in the hyperphosphorylation of paired helical filament-tau (Ishiguro *et al.* 1993; Morishima-Kawashima *et al.* 1995; Goedert *et al.* 1997), GSK-3 β and JNK hyperphosphorylation leads to the formation of paired helical filament-like, detergent-insoluble tau (Sato *et al.* 2002). Tau gene mutations have recently been reported to cause frontotemporal dementia with parkinsonism-17, which has been characterized as exhibiting NFTs and neuron loss

without β -amyloid peptide deposition in autopsied human brains, demonstrating that tau abnormalities alone can cause NFTs and neuronal death. While exonic mutations, such as P301L, affect the biochemical nature of tau and promote the self-assembly of mutant tau into filaments, intronic mutations within exon 10 or its 5' splice regulatory region alter the ratio

Received January 19, 2004; revised manuscript received May 27, 2004; accepted June 11, 2004.

Address correspondence and reprint requests to Akihiko Takashima, Laboratory for Alzheimer's Disease, Brain Science Institute, RIKEN, Saitama 351-0198, Japan. E-mail: kenneth@brain.riken.jp

Abbreviations used: AD, Alzheimer's disease; CHIP, carboxyl terminus of Hsc70-interacting protein; EGFP, enhanced green fluorescent protein; GFP, green fluorescent protein; GST, glutathione S-transferase; HA, haemagglutinin; IB, immunoblot; IP, immunoprecipitate; NFT, neurofibrillary tangle; RNAi, RNA interference; SDS, sodium dodecyl sulfate; TPR, tetratricopeptide repeat; WCE, whole cell lysate.

of tau isoforms. In general, these mutations affect exon 10 splicing patterns thus altering the relative proportions of four- and three-repeat tau that are expressed. An increase in four-repeat tau induces the accumulation of four-repeat tau and NFT formation. We assumed that an impairment in a mechanism for four-repeat tau degradation would lead to four-repeat tau accumulation. As tau in NFTs is ubiquitinated, the ubiquitin proteasome may be the mechanism responsible for tau degradation in neurodegeneration (Mori *et al.* 1987) and the deterioration of this system might contribute to NFT formation. However, the mechanism by which the ubiquitylation of tau occurs is still unknown.

Protein ubiquitylation is mediated by a multienzyme cascade involving at least three distinct types of enzymes, a ubiquitin-activating enzyme (E1), a ubiquitin-conjugating enzyme (E2) and a ubiquitin-protein ligase (E3) (Hershko 1983). E3 enzymes catalyse the final step for substrate recognition in the ubiquitylation pathway. Currently there are two known E3 ligases, the HECT family E3s and adaptor E3s containing a RING finger or a U-box (Weissman 2001; Hatakeyama and Nakayama 2003). The carboxyl terminus of Hsc70-interacting protein (CHIP) has a U-box domain and was originally identified as a tetratricopeptide repeat (TPR)-containing protein that interacts with mammalian heat shock protein Hsc/Hsp70 (Ballinger *et al.* 1999). CHIP binds directly to the molecular chaperones Hsp90 or Hsc70 via TPR domains; therefore, when unfolded or misfolded proteins accumulate, CHIP may contribute to the cellular response. The combination of CHIP and Hsp90 mediates the ubiquitylation of the glucocorticoid receptor and CHIP with Hsc70 targets the immature cystic fibrosis transmembrane conductance regulator for proteasomal degradation (Connell *et al.* 2001; Meacham *et al.* 2001). We recently showed that the level of Hsp90 is reduced in tau-accumulated neurons of Tg mice expressing frontotemporal dementia with parkinsonism-17 tau mutations (Tanemura *et al.* 2001, 2002; Tatebayashi *et al.* 2002; Dou *et al.* 2003). This prompted us to investigate the possible involvement of CHIP in the poly-ubiquitylation of tau.

Materials and methods

Cell culture

HEK293T, COS7 or Neuro2A cells were cultured under an atmosphere of 5% CO₂ at 37°C in Dulbecco's modified Eagle's medium (Invitrogen; Carlsbad, CA, USA) supplemented with 10% fetal bovine serum (Invitrogen).

Cloning cDNAs and plasmid construction

The expression plasmids containing FLAG- or Myc-tagged mouse CHIP, mutants of these cDNAs [UFD2a, UFD2b, PRP19, IκBα, IKK2, haemagglutinin (HA)-tagged ubiquitin and wild type (four- and three-repeat)] and tau mutants were generated as previously

described (Hatakeyama *et al.* 2001). To generate the mutant (P301L) of tau or Hsc70, we performed site-directed mutagenesis with a Quick Change kit (Stratagene, La Jolla, CA, USA) and with mutated oligonucleotide primers corresponding to each site.

Production of recombinant proteins in bacteria

Glutathione S-transferase (GST) fusion proteins were expressed in *Escherichia coli* strain DH5α cultured in the presence of 0.1 mM isopropyl-β-D-thiogalactopyranoside. Bacterial cells were resuspended in phosphate-buffered saline and lysed by sonication; cellular debris was removed by centrifugation for 20 min at 13 000 g. Glutathione-Sepharose 4B beads (Amersham Biosciences, Piscataway, NJ, USA) were added to the resulting supernatant fluid and the mixture was rotated at 4°C overnight. The beads were washed in phosphate-buffered saline and GST fusion proteins were eluted with 50 mM Tris-HCl (pH 8.0) containing 10 mM reduced glutathione.

Transfection, immunoprecipitation and immunoblot analysis

Cells were transfected using the calcium phosphate method and lysed in a lysis buffer containing 50 mM Tris-HCl (pH 7.4), 150 mM NaCl, 1% nonidet P-40, leupeptin (10 µg/mL), 1 mM phenylmethylsulfonyl fluoride, 400 µM Na₂VO₄, 400 µM EDTA, 1 mM EGTA, 10 mM NaF and 10 mM sodium pyrophosphate. The lysate was centrifuged at 16 000 g for 10 min at 4°C and the resulting supernatant fluid was incubated with antibodies for 2 h at 4°C. Protein G-Sepharose equilibrated in the same buffer was added to the mixture, which was then rotated for 1 h at 4°C. The resin was separated by centrifugation, washed four times with lysis buffer and then boiled in sodium dodecyl sulfate (SDS) sample buffer. Immunoblot analysis was performed with the following primary antibodies: anti-Myc (1 µg/mL; 9E10, Covance Inc., Princeton, NJ, USA), anti-FLAG (1 µg/mL; M5, Sigma-Aldrich, St. Louis, MO, USA), anti-HA (1 µg/mL; HA.11/16B12, Babco, Berkeley, CA, USA), anti-Hsp90 (1 µg/mL; 68, Transduction Laboratories, San Jose, CA, USA), anti-Hsp70 (1 µg/mL; 7, Transduction Laboratories), anti-CHIP (1 µg/mL, Hatakeyama and Nakayama 2003), p27^{Kip1} (1 µg/mL; 57, Transduction Laboratories) and anti-ubiquitin (1 µg/mL; 1B3, MBL International, Woburn, MA, USA). Immune complexes were detected with horseradish peroxidase-conjugated antibodies to mouse or rabbit immunoglobulin G (1 : 10 000 dilution; Promega Corporation, Madison, WI, USA) and an enhanced chemiluminescence system (ECL; Amersham Biosciences).

Isolation of insoluble tau from cell lines

Cells were lysed with ristocetin-induced platelet agglutination buffer containing 1% SDS. Cell lysate (2 mg) was centrifuged for 20 min at 100 000 g at 4°C. The resulting pellet was washed four times with 300 µL of ristocetin-induced platelet agglutination buffer using a sonic homogenizer. The insoluble pellet was solubilized in 70% formic acid for use in the immunoblot analysis or resuspended in 100 mM Tris-HCl (pH 8.3) for examination using electron microscopy. Following centrifugation for 20 min at 100 000 g at 4°C, the formic acid fraction was collected, air-dried and subjected to immunoblot analysis after suspension in SDS gel loading buffer. The samples were resolved on SDS-polyacrylamide gel electrophoresis and immunoblot analysis was performed.

In vitro ubiquitylation assay

The *in vitro* ubiquitylation assay was performed as described previously (Hatakeyama *et al.* 2001). In brief, reaction mixtures (20 μ L) containing 1 μ g of recombinant GST-CHIP, 0.1 μ g of recombinant rabbit E1 (Boston Biomedica, Boston, MA, USA), 1 μ L of recombinant human Ubc4, 0.5 U of phosphocreatine kinase, 1 μ g of GST-Ub (MBL), 25 mM Tris-HCl (pH 7.5), 120 mM NaCl, 2 mM ATP, 1 mM MgCl₂, 0.3 mM dithiothreitol and 1 mM creatine phosphate were incubated for 2 h at 30°C. The reaction was terminated by the addition of SDS sample buffer containing 4% 2ME and heating at 95°C for 5 min. Samples were resolved by SDS-polyacrylamide gel electrophoresis on a 6% gel and then subjected to immunoblot analysis with a mouse monoclonal antibody to tau (clone 15; Transduction Laboratories) and horseradish peroxidase-conjugated rabbit polyclonal antibody to mouse Ig (Promega). Signals were detected with ECL (Amersham Pharmacia).

Pulse-chase analysis with cycloheximide

Cells were cultured with cycloheximide at a concentration of 50 μ g/mL and then incubated for various times. Cell lysates were then subjected to SDS-polyacrylamide gel electrophoresis and immunoblot analysis with antibody to Myc, Hsp90, FLAG and p27^{Kip1}.

RNA interference and retroviral infection

The retroviral expression vector, which encodes the double-stranded RNA corresponding to nucleotides 864–883 of the mouse CHIP coding region or to enhanced green fluorescent protein (EGFP), was constructed using pMX-puro, kindly provided by Dr Kitamura (Osaka University, Graduate School of Medicine, Osaka, Japan). For retrovirus-mediated gene expression, Neuro2A cells were infected with retroviruses produced by Plat-E packaging cells and then cultured in the presence of 0.2 μ g/mL puromycin (Sigma). pMX-neo vector was used for Myc-tau (P301L).

Induction and detection of cell death

Stable Neuro2A cell lines were cultured with 20 μ M MG132 (Peptide Institute, Osaka, Japan) and incubated for 24 h; the cell number was counted after trypan blue staining.

Immunohistochemical staining

Brains were immersion fixed with 10% buffered formalin and paraffin-embedded sections (2–10 μ m) were prepared for confocal microscopic analyses. Deparaffinized sections were treated in either 0.1% Triton X-100 in phosphate-buffered saline for 20 min or Target Retrieval Solution (Dako Cytomation Denmark A/S, Glostrup, Denmark). AT8 and anti-CHIP were used as primary antibodies and then incubated with either Alexa488/568-conjugated anti-mouse IgG or Alexa488/568-conjugated anti-rabbit IgG. Sections were then examined with a Radiance 2000 KR3 confocal microscope (Bio-Rad Laboratories, Hercules, CA, USA).

Results

We first examined the involvement of U-box proteins in tau ubiquitylation. The overexpression of UFD2a, UFD2b or PRP19 U-box proteins had no effect on tau ubiquitylation compared with control, which showed only minimal tau

ubiquitylation with endogenous E3 ligases (Fig. 1a). Only CHIP overexpression exhibited poly-ubiquitylated tau (Fig. 1a), suggesting that CHIP participates in this ubiquitylation process. To confirm this result, various combinations of tau, Myc-CHIP and HA-tagged ubiquitin were expressed in COS7 cells and tau was purified from the heat-stable materials of each cell lysate by immunoprecipitation using an anti-tau antibody. Tau from Myc-CHIP- and HA-tagged ubiquitin-coexpressing cells revealed anti-HA immunoreactivity, suggesting that tau protein is covalently modified by ubiquitin under the expression of CHIP (Fig. 1b). This result was verified by purifying ubiquitylated protein from CHIP- and tau-expressing cells. Using an Ni column, ubiquitylated proteins were purified from cells expressing tau, histidine-tagged Ub with or without CHIP. CHIP expression greatly enhanced the recovery of ubiquitylated tau in elution fractions 1 and 2 (Fig. 1c) and the ubiquitylated tau by CHIP was about 3.4% of total tau. Thus, CHIP is an E3-ubiquitin ligase for tau and the overexpression of CHIP increases tau ubiquitylation in an *in vivo* system. To further confirm the ubiquitylation of tau by CHIP, we reconstituted ubiquitylated tau in an *in vitro* ubiquitylation assay with these recombinants; E1, E2 (UbcH5C), GST-ubiquitin (GST-Ub), GST-CHIP and His-tau were required for tau ubiquitylation (Fig. 1d). Unexpectedly, chaperone proteins, phosphorylated tau or other such factors were not required for tau ubiquitylation by CHIP. Thus, these results indicated that CHIP alone can ubiquitylate even non-phosphorylated tau *in vitro*.

To test the interaction between tau and CHIP *in vivo*, mutants with CHIP and tau deletions (Fig. 2) were prepared and expressed in HEK293 or COS7 cells. Full-length tau could bind to full-length CHIP but not to CHIP (Δ U) lacking a U-box domain, CHIP (Δ TPR) lacking a TPR or CHIP (Δ CU) lacking both the charged region and U-box (Fig. 2a). Conversely, full-length CHIP could associate with full-length tau (four-repeat) and with the region lacking the N-terminus of tau (R-C) but not with the region lacking the repeat regions (Δ R) (Fig. 2b). These findings suggest that CHIP associates with the microtubule-binding repeat regions of tau. We further investigated the interaction and ubiquitylation of CHIP on four- and three-repeat tau (Fig. 2c). Three-repeat tau was less efficiently ubiquitylated by CHIP (Fig. 2d) and the association of three-repeat tau and CHIP was much less than for four-repeat tau (Fig. 2c). Thus, CHIP might recognize around the second repeat region of tau, which corresponds to exon 10 and preferentially ubiquitylates four-repeat tau.

We next investigated the effects of CHIP on the stability of tau in Neuro2A cells stably expressing Myc-tau (P301L) and FLAG-CHIP (Fig. 3a). The stability of tau (P301L) was examined by cyclohexamide-chase analysis. After cycloheximide treatment, endogenous p27^{Kip1} protein rapidly degraded (Fig. 3a, two blots from bottom) and endogenous HSP90 protein remained stable for over 30 h (Fig. 3a, third and

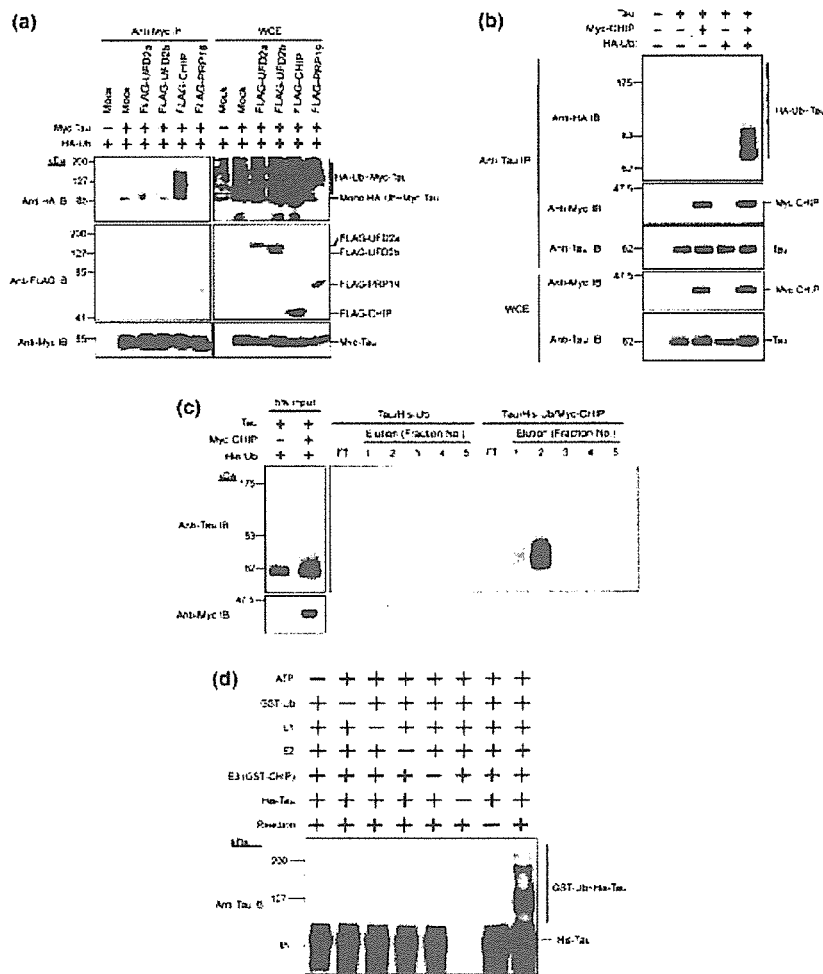


Fig. 1 Carboxyl terminus of Hsc70-interacting protein (CHIP) expression enhances the ubiquitylation on tau *in vivo*. (a) Specific ubiquitin ligase activity of CHIP for tau. The expression vectors for FLAG-UFD2a, -UFD2b, -CHIP, -PRP19, Myc-tagged human four-repeat tau and HA-tagged ubiquitin (HA-Ub) were transfected into HEK293T cells, the cell lysates were immunoprecipitated with anti-Myc monoclonal antibody and an anti-HA immunoblot was performed to detect the ubiquitylation on tau. Ten percent of cell lysates were used as WCE to detect the expression of each protein. (b) *In vivo* ubiquitylation assay for tau with CHIP. The expression vectors for Myc-CHIP, tau and HA-Ub were transfected into COS7 cells, the cell lysates were then immunoprecipitated with anti-tau monoclonal antibody and an anti-HA immunoblot was performed to detect the ubiquitylation on tau.

Ten percent of cell lysates were used as WCE to detect the expression of each protein. (c) Fractionation of ubiquitylated tau from a cell expressing CHIP. The expression vectors for Myc-CHIP, tau and HA-Ub were transfected into COS7 cells, the cell lysates were then fractionated using an Ni column and an anti-tau immunoblot was performed to detect the ubiquitylation on tau. Five percent of cell lysates were used as WCE to detect the expression of each protein. (d) *In vitro* ubiquitylation assay for tau with CHIP. Each component [ATP, glutathione S-transferase (GST)-Ub, E1, Ubc4, GST-CHIP and His-tau] was mixed, incubated at 30°C for 2 h, subjected to sodium dodecyl sulfate–polyacrylamide gel electrophoresis and then immunoblotted with anti-tau monoclonal antibody. IB, immunoblot; IP, immunoprecipitate; WCE, whole cell lysate.

fourth blots from top) when CHIP and tau were overexpressed together (Fig. 3a, third and seventh blots) and when tau alone was overexpressed (Fig. 3a, fourth and eighth blots from the top). Tau remained stable for over 30 h only in cells overexpressing tau (Fig. 3a, first blot), whereas the overexpression of CHIP enhanced tau degradation (Fig. 3a, second blot) without changing the exogenous expression level of CHIP (Fig. 3a, sixth blot from top). Moreover, tau ubiquitylated by CHIP accumulated when treated with the protea-

some inhibitor lactacystin (Fig. 3b) These results suggest that CHIP induces the ubiquitylation of tau which is followed by degradation via proteasome. The effects of CHIP on the stability and ubiquitination of tau were not different between the P301L mutant and wild tau.

Knowing that CHIP recognizes and ubiquitylates tau and that this is followed by proteasome degradation, we investigated the role of CHIP in SDS-insoluble tau formation, one of the biochemical features of paired

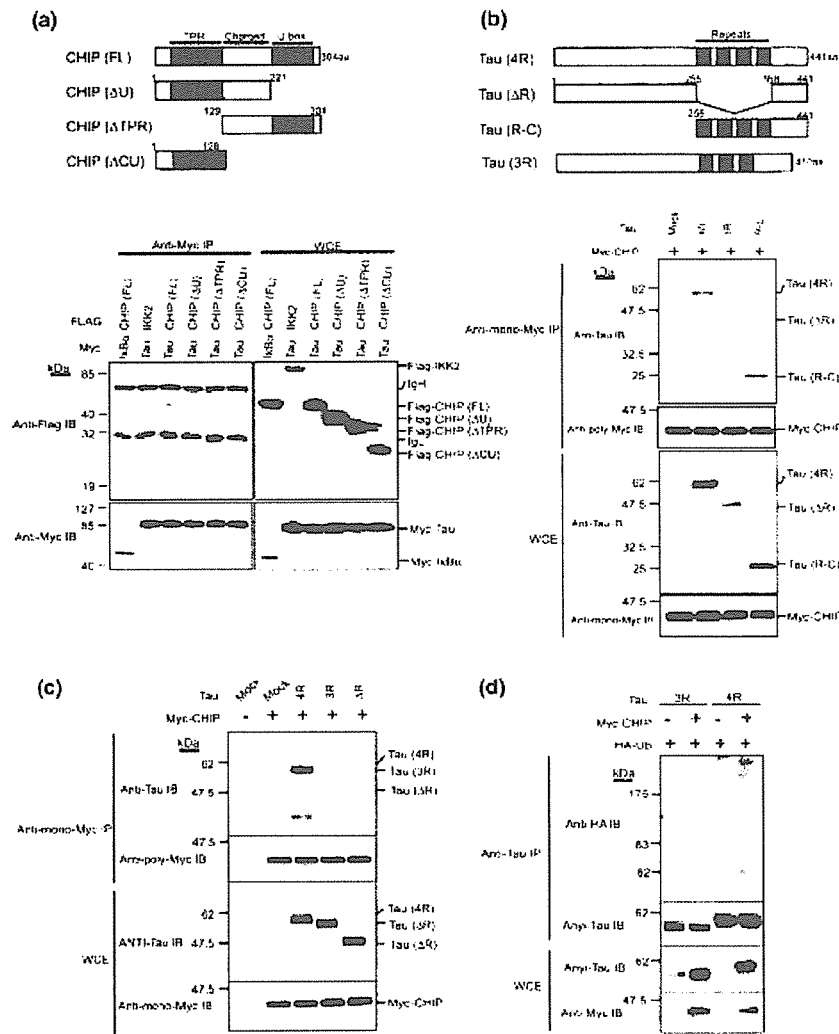


Fig. 2 Interaction between carboxyl terminus of Hsc70-interacting protein (CHIP) and four-repeat (4R) tau. (a) *In vivo* interaction between CHIP and tau. CHIP (FL) has the full-length (1–304) of CHIP. CHIP (ΔU), CHIP (ΔTPR) and CHIP (ΔCU) contain deletions of the U-box domain (222–304), tetratricopeptide repeat (TPR) domain (1–128) and charged region plus U-box domain (129–304), respectively. Black and gray boxes show the TPR and U-box domains, respectively. The expression vectors for full-length and mutants of FLAG-CHIP and Myc-tau (4R) were transfected into HEK293T cells, the cell lysates were immunoprecipitated with anti-Myc monoclonal antibody and anti-FLAG immunoblot was performed to detect the association with FLAG-CHIP or its mutants. Ten percent of cell lysates were used as WCE to detect the expression of each protein. Myc-IκBα and FLAG-IKK were used for negative controls. (b) Repeat domain of 4R tau interacts with CHIP. Tau (4R) is the longest form of 4R tau. Tau (ΔR) and tau (R-C) are the deletion of the 4R domain (256–441) and the N-terminal half (1–255), respectively. Black box shows repeat domain. The expression vectors for Myc-CHIP and truncated tau (4R) were transfected into COS7 cells,

the cell lysates were immunoprecipitated with anti-Myc monoclonal antibody and anti-tau immunoblot was performed to detect the association with Myc-CHIP. The amount of immunoprecipitated CHIP was the same in all cell lysates (bottom panel). Ten percent of cell lysates were used as WCE to detect the expression of each protein. (c) Association of CHIP with 4R and three-repeat tau (3R). cDNAs described on the top of the blots were transfected into COS7 cells and cell lysates were immunoprecipitated using anti-myc antibody. Immunoprecipitants were probed by the anti-tau antibody TauC or anti-polyclonal antibody Myc. The amount of immunoprecipitated CHIP was the same in all cell lysates (bottom panel). (d) Ubiquitylation of 4R and 3R tau by CHIP. Each combination of cDNAs was transfected into COS7 cells. After immunoprecipitation of heat-stable materials using anti-tau antibody (HT7), immunoprecipitants were probed by anti-HA or tau C. The amount of immunoprecipitated tau was the same in all cell lysates (anti-tau IB panel in anti-tau IP panels) while the tau expression level was different.

helical filament-tau, using Neuro2A coexpressing fronto-temporal dementia with parkinsonism-17 mutant tau (P301L) with or without FLAG-CHIP. The expression of

P301L mutant tau induced the formation of SDS-insoluble tau and enhanced the recovery of tau in the SDS-insoluble fraction (formic acid-soluble fraction) by treatment with

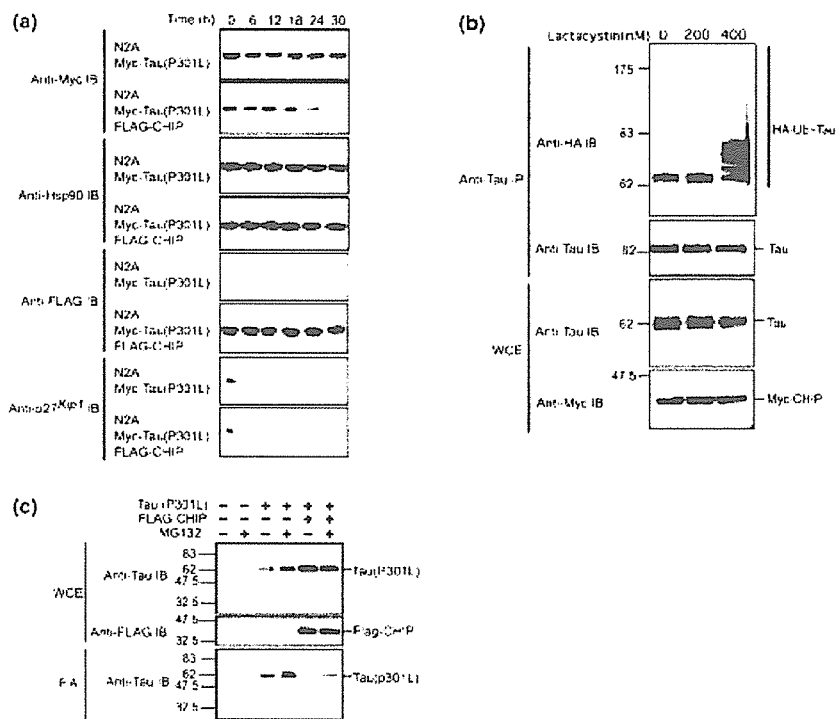


Fig. 3 Carboxyl terminus of Hsc70-interacting protein (CHIP) implicated in the regulation of neuronal cell death. (a) Cycloheximide-chase analysis of tau (P301L) with CHIP. The stably expressed Neuro2A cell lines with Myc-tau (P301L) and FLAG-CHIP were established by infection of retrovirus with cDNA encoding Myc-tau (P301L) and FLAG-CHIP and by puromycin selection. Cells were cultured with cycloheximide at a concentration of 50 μg/mL and then incubated for various times (0, 6, 12, 18, 24 and 30 h). Cell lysates were then subjected to sodium dodecyl sulfate–polyacrylamide gel electrophoresis (SDS–PAGE) and immunoblot analysis was performed with antibody to Myc, Hsp90, FLAG and p27^{Kip1}. The anti-p27^{Kip1} immunoblot shows that

cycloheximide is active. (b) Effects of treatment with the proteasome inhibitor lactacystin. HEK293 cells expressing tau, CHIP and HA-tagged ubiquitin (HA-Ub) were treated with various concentrations of lactacystin for 14 h, the cell lysates were immunoprecipitated with anti-tau monoclonal antibody and an anti-HA immunoblot was performed to detect the ubiquitylation on tau. (c) Soluble or insoluble fraction of Tau (P301L). The soluble (WCE) or insoluble [formic acid (FA)] fraction from cells expressing Tau (P301L) with or without FLAG-CHIP was separated with or without treatment with MG135. The fractions were subjected to SDS–PAGE and immunoblot analysis was performed with antibody to tau and FLAG. Hsp90 as internal control.

MG132, a potent inhibitor of proteasome (Fig. 3c, lanes 3 and 4). Coexpression with CHIP sustained the amount of the SDS-soluble tau fraction and significantly inhibited the formation of SDS-insoluble tau. MG132 treatment enhanced the formation of SDS-insoluble tau but the amount recovered was still much lower than that from cells where CHIP was not coexpressed (Fig. 3c, lanes 5 and 6). These results indicate that the inhibition of SDS-insoluble tau formation stems from the role of CHIP in the degradation of tau. Thus, CHIP may be involved in NFT formation.

Many suspect a possible connection between NFT formation and neuronal death in neurodegenerative diseases because neuronal loss is also common in areas where NFTs are observed. Therefore, we investigated the possible role of CHIP in connecting NFT formation and cell death. We first established cell lines that knocked down endogenous CHIP using a vector-based RNA interference (RNAi) technique (Fig. 4a). CHIP RNAi expression blocked the expression of

endogenous CHIP but did not affect the expression of Hsp90. Green fluorescent protein (GFP) RNAi also did not affect CHIP expression. Tau (P301) over-expression had no effect on the cell viability of Neuro2A, even though SDS-insoluble tau was formed. Stable cell lines were incubated with the proteasome inhibitor MG132 (20 μM) for 24 h and then alive or dead cells were determined by trypan blue exclusion (Fig. 4b). This treatment induced cell death in 50% of the non-treated cells in GFP RNAi-expressing cells, CHIP-overexpressing cells and mock cells. The RNAi inhibition of CHIP and the expression of tau (P301L) facilitated an MG132-induced cell death of 70% of untreated cells and CHIP overexpression restored the cell death level to that of cells with no tau expression (Fig. 4b). Therefore, CHIP is involved in tau (P301L)-mediated, MG132-induced cell death. It should be noted that, although CHIP expression prevented neurons from undergoing proteasome inhibition-induced neuronal death, surviving neurons still showed SDS-insoluble tau (Fig. 3c) which suggests the development of

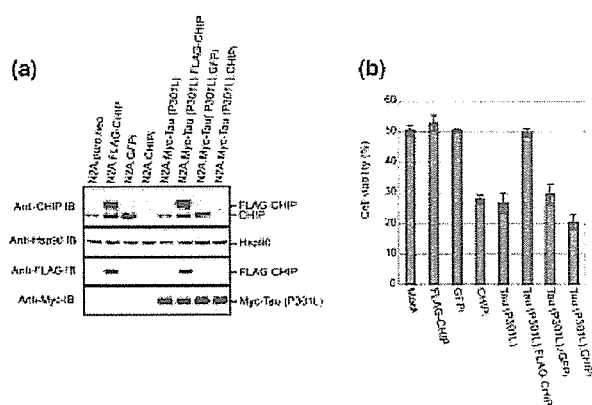


Fig. 4 Carboxyl terminus of Hsc70-interacting protein (CHIP) as a critical factor to protect from stress by proteasome inhibitor. (a) Reduced amounts of CHIP in cells with CHIP RNA interference (RNAi) but not EGFP RNAi. Neuro2A cells were treated with retrovirus vector-based RNAi for CHIP or EGFP and then selected with puromycin. These cell lines were further infected by retrovirus with Myc-tau (P031L) and neo^R and then selected with puromycin and G418. Double-infected cell lines were used for immunoblot with antibodies to CHIP, FLAG, Myc and Hsp90 as internal control. (b) Stable Neuro2A cell lines were cultured with 20 μ M MG132, incubated for 24 h and the cell number was counted after trypan blue staining. The amounts of CHIP in cells with CHIP but not EGFP RNAi were reduced. Neuro2A cells were treated with retrovirus vector-based RNAi for CHIP or EGFP and then selected with puromycin.

NFT formation. This was verified by neuropathological staining in which CHIP colocalized in NFTs of progressive supranuclear palsy brain (Fig. 5), mostly containing four-repeat tau, and also reacted to anti-ubiquitin antibody. The most NFT-bearing cells were stained by the anti-CHIP antibody in progressive supranuclear palsy brain but very faintly stained in Alzheimer's disease (AD) brain (data not shown).

Discussion

In this study, we have shown that the U-box protein CHIP is a tau-interacting protein *in vivo* and that CHIP mediates poly-ubiquitylation preferentially on four-repeat tau as a ubiquitin ligase followed by degradation by proteasome. In the *in vitro* ubiquitylation assay, molecular chaperones such as Hsp90 or Hsc70 or hyperphosphorylation of tau are not required for CHIP-mediated tau ubiquitylation (Fig. 1d). To date, CHIP has been shown to bind to a subset of chaperone substrates, including glucocorticoid receptor, cystic fibrosis transmembrane conductance regulator and ErbB2, suggesting that CHIP has sensor functions that recognize different kinds of misfolded proteins (Connell *et al.* 2001; Meacham *et al.* 2001; Imai *et al.* 2002; Xu *et al.* 2002). In *in vivo* conditions, Hsp might support the CHIP-mediated tau ubiquitylation and degradation because tau was not accumulated in neurons exhibiting an increased level of Hsp90 (Dou *et al.* 2003). To

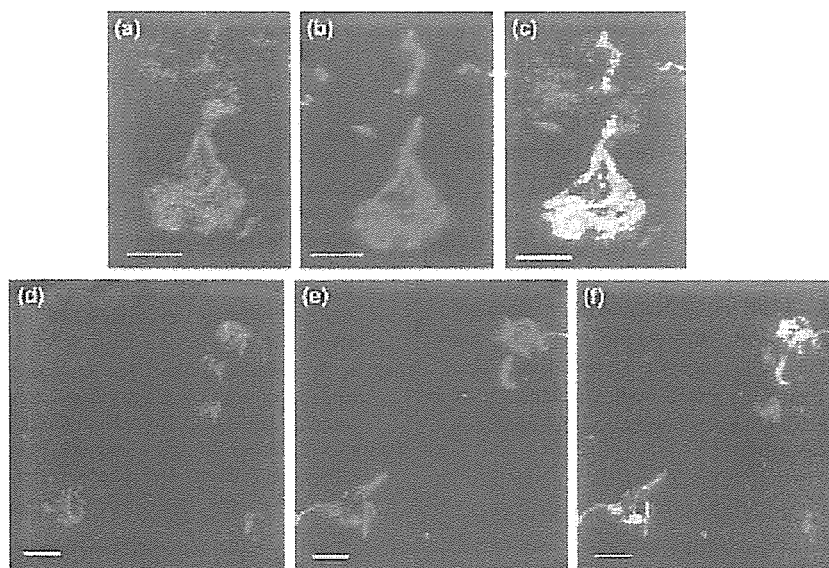


Fig. 5 Neuropathological analysis in progressive supranuclear palsy (PSP). Neurons in PSP brain were stained with anti-carboxyl terminus of Hsc70-interacting protein (CHIP; green; a and d) and anti-phosphorylated tau (AT8; orange; b and e). (c and f) Merged image of both anti-CHIP and AT8 immunoreactivities. Brains were immersion fixed with 10% buffered formalin and paraffin-embedded sections (2–10 μ m) were prepared for confocal microscopic analyses.

Deparaffinized sections were treated in either 0.1% Triton X-100 in phosphate-buffered saline for 20 min or Target Retrieval Solution (Dako). AT8 and anti-CHIP were used as primary antibodies and then incubated with either Alexa488/568-conjugated anti-mouse IgG or Alexa488/568-conjugated anti-rabbit IgG. Sections were then examined with a Radiance 2000 KR3 confocal microscope (Bio-Rad). Scale bars, 10 μ m.

uncover how CHIP recognizes and ubiquitylates tau without molecular chaperones, it is first necessary to understand the structural basis for this significant function.

Phosphorylated tau was reported to preferentially ubiquitylate in COS cells (Shimura *et al.* 2003). In our experiments, four-repeat tau was ubiquitylated by CHIP without phosphorylation. This discrepancy might be due to the different purification procedures for ubiquitylated tau and/or the different tau cDNA used. Shimura *et al.* (2003) used EGFP-tagged tau. As recombinant tau, which was not phosphorylated, could be ubiquitylated in an *in vitro* reconstitution system, CHIP must recognize and ubiquitylate both non-phospho and phospho tau.

The ubiquitinated tau found in AD brains was recovered in the SDS-insoluble fraction, suggesting that its ubiquitylation may precede fibril formation. A large amount of SDS-insoluble tau was recovered in P301L mutant tau-expressing cells in the present study and MG132 treatment enhanced the accumulation of tau in the SDS-insoluble fraction, suggesting that tau (P301L) is degraded by the ubiquitin-proteasome system. CHIP overexpression reduced the recovery of tau in the SDS-insoluble fraction and MG132 treatment showed only a small increase of SDS-insoluble tau, suggesting that the ubiquitylation of tau occurs before tau acquires insolubility against SDS. An inhibition of proteasome activity in the AD brain has been reported previously (Goldbaum *et al.* 2003; Keck *et al.* 2003). Taken together with the MG132-induced cytotoxicity of P301L tau overexpression, these results suggest that tau accumulation in the SDS-insoluble fraction itself was not toxic but rather that the neurons exhibited vulnerability against the stress of protein accumulation by inhibition of proteasome. CHIP expression reduces the stress induced by this cytotoxicity by reducing the amount of SDS-insoluble tau. Therefore, although CHIP-expressing neurons survive, ubiquitylated tau might remain in some neurons and develop into NFTs.

Acknowledgements

We thank S. Matsushita, K. Shinohara, N. Nishimura, R. Yasukouchi and other laboratory members for technical assistance and C. Sugita and M. Kimura for help in preparing the manuscript. This work was supported in part by a grant from the Ministry of Education, Science, Sports and Culture of Japan and by YASUDA Medical Research Foundation (SH).

References

- Ballinger C. A., Connell P., Wu Y., Hu Z., Thompson L. J., Yin L. Y. and Patterson C. (1999) Identification of CHIP, a novel tetratricopeptide repeat-containing protein that interacts with heat shock proteins and negatively regulates chaperone functions. *Mol. Cell. Biol.* **19**, 4535–4545.
- Connell P., Ballinger C. A., Jiang J., Wu Y., Thompson L. J., Hohfeld J. and Patterson C. (2001) The co-chaperone CHIP regulates protein triage decisions mediated by heat-shock proteins. *Nat. Cell Biol.* **3**, 93–96.
- Dou F., Netzer W. J., Tanemura K., Li F., Hartl F. U., Takashima A., Gouras G. K., Greengard P. and Xu H. (2003) Chaperones increase association of tau protein with microtubules. *Proc. Natl Acad. Sci. USA* **100**, 721–726.
- Goedert M., Hasegawa M., Jakes R., Lawler S., Cuenda A. and Cohen P. (1997) Phosphorylation of microtubule-associated protein tau by stress-activated protein kinases. *FEBS Lett.* **409**, 57–62.
- Goldbaum O., Oppermann M., Handschuh M., Dabir D., Zhang B., Forman M. S., Trojanowski J. Q., Lee V. M. and Richter-Landsberg C. (2003) Proteasome inhibition stabilizes tau inclusions in oligodendroglial cells that occur after treatment with okadaic acid. *J. Neurosci.* **23**, 8872–8880.
- Hardy J. and Selkoe D. J. (2002) The amyloid hypothesis of Alzheimer's disease: progress and problems on the road to therapeutics. *Science* **297**, 353–356.
- Hatakeyama S. and Nakayama K. I. (2003) U-box proteins as a new family of ubiquitin ligases. *Biochem. Biophys. Res. Commun.* **302**, 635–645.
- Hatakeyama S., Yada M., Matsumoto M., Ishida N. and Nakayama K. I. (2001) U box proteins as a new family of ubiquitin-protein ligases. *J. Biol. Chem.* **276**, 33 111–33 120.
- Hershko A. (1983) Ubiquitin: roles in protein modification and breakdown. *Cell* **34**, 11–12.
- Imai Y., Soda M., Hatakeyama S., Akagi T., Hashikawa T., Nakayama K. and Takahashi R. (2002) CHIP is associated with Parkin, a gene responsible for familial Parkinson's disease, and enhances its ubiquitin ligase activity. *Mol. Cell* **10**, 55–67.
- Ishiguro K., Shiratsuchi A., Sato S., Omori A., Arioka M., Kobayashi S., Uchida T. and Imahori K. (1993) Glycogen synthase kinase 3 beta is identical to tau protein kinase I generating several epitopes of paired helical filaments. *FEBS Lett.* **325**, 167–172.
- Keck S., Nitsch R., Grune T. and Ullrich O. (2003) Proteasome inhibition by paired helical filament-tau in brains of patients with Alzheimer's disease. *J. Neurochem.* **85**, 115–122.
- Kopito R. R. and Ron D. (2000) Conformational disease. *Nat. Cell Biol.* **2**, E207–E209.
- Lee V. M., Goedert M. and Trojanowski J. Q. (2001) Neurodegenerative tauopathies. *Annu. Rev. Neurosci.* **24**, 1121–1159.
- Meacham G. C., Patterson C., Zhang W., Younger J. M. and Cyr D. M. (2001) The Hsc70 co-chaperone CHIP targets immature CFTR for proteasomal degradation. *Nat. Cell Biol.* **3**, 100–105.
- Mori H., Kondo J. and Ihara Y. (1987) Ubiquitin is a component of paired helical filaments in Alzheimer's disease. *Science* **235**, 1641–1644.
- Morishima-Kawashima M., Hasegawa M., Takio K., Suzuki M., Yoshida H., Titani K. and Ihara Y. (1995) Proline-directed and non-proline-directed phosphorylation of PHF-tau. *J. Biol. Chem.* **270**, 823–829.
- Sato S., Tatebayashi Y., Akagi T. *et al.* (2002) Aberrant tau phosphorylation by glycogen synthase kinase-3beta and JNK3 induces oligomeric tau fibrils in COS-7 cells. *J. Biol. Chem.* **277**, 42 060–42 065.
- Selkoe D. J. (2000) Toward a comprehensive theory for Alzheimer's disease. Hypothesis: Alzheimer's disease is caused by the cerebral accumulation and cytotoxicity of amyloid beta-protein. *Ann. NY Acad. Sci.* **924**, 17–25.
- Shimura H., Schwartz D., Gygi S. P. and Kosik K. S. (2004) CHIP-Hsc70 complex ubiquitinates phosphorylated Tau and enhances cell survival. *J. Biol. Chem.* **279**, 4869–4876.
- Tanemura K., Akagi T., Murayama M. *et al.* (2001) Formation of filamentous tau aggregations in transgenic mice expressing V337M human tau. *Neurobiol. Dis.* **8**, 1036–1045.
- Tanemura K., Murayama M., Akagi T., Hashikawa T., Tominaga T., Ichikawa M., Yamaguchi H. and Takashima A. (2002) Neurode-

- generation with tau accumulation in a transgenic mouse expressing V337M human tau. *J. Neurosci.* **22**, 133–141.
- Tatebayashi Y., Miyasaka T., Chui D. H. *et al.* (2002) Tau filament formation and associative memory deficit in aged mice expressing mutant (R406W) human tau. *Proc. Natl Acad. Sci. USA* **99**, 13 896–13 901.
- Weissman A. M. (2001) Themes and variations on ubiquitylation. *Nat. Rev. Mol. Cell Biol.* **2**, 169–178.
- Xu W., Marcu M., Yuan X., Minnaugh E., Patterson C. and Neckers L. (2002) Chaperone-dependent E3 ubiquitin ligase CHIP mediates a degradative pathway for c-ErbB2/Neu. *Proc. Natl Acad. Sci. USA* **99**, 12 847–12 852.



How do Parkin mutations result in neurodegeneration?

Yuzuru Imai and Ryosuke Takahashi

The gene product responsible for autosomal recessive juvenile Parkinsonism, Parkin, has been observed to have ubiquitin ligase activity. This finding has changed the direction of studies on Parkinson's disease by suggesting that abnormal protein turnover might be involved in its pathogenesis. A number of potentially neurotoxic Parkin-specific substrates have been identified. Further investigation of Parkin knockout mice will hopefully provide new evidence in the search for Parkin's substrates and further clarify their role in Parkinson's disease.

Addresses

Motor System Neurodegeneration, RIKEN Brain Science Institute (BSI),
Saitama 351-0198, Japan
e-mail: ryosuke@brain.riken.jp

Current Opinion in Neurobiology 2004, 14:384–389

This review comes from a themed issue on
Signalling mechanisms
Edited by Richard L Haganir and S Lawrence Zipursky

Available online 30th April 2004

0959-4388/\$ – see front matter
© 2004 Elsevier Ltd. All rights reserved.

DOI 10.1016/j.conb.2004.04.002

Abbreviations

AR-JP	autosomal recessive juvenile Parkinsonism
CDCrel-1	cell division control-related protein 1
CHIP	carboxy-terminus of Hsc70-interacting protein
E3	ubiquitin ligase
Hsp	heat shock protein
LB	Lewy body
Pael-R	Pael receptor
PD	Parkinson's disease
RING	really interesting new gene
TH	tyrosine hydroxylase
Ubl	ubiquitin-like domain

Introduction

Parkinson's disease (PD) is a movement disorder characterized by a progressive loss of dopaminergic neurons in the substantia nigra pars compacta. As in most cases of PD the degeneration is idiopathic, the etiology of the disease remains unknown. The recent identification of genetic mutations in familial cases of PD has advanced our understanding of the molecular mechanisms that cause the neurodegeneration.

Two rare missense mutations in the α -synuclein gene (A53T and A30P) cause autosomal dominant familial PD [1,2]. Although the physiological function of α -synuclein is still unclear, there is evidence that even wild type α -synuclein is a major component of Lewy bodies (LBs) and

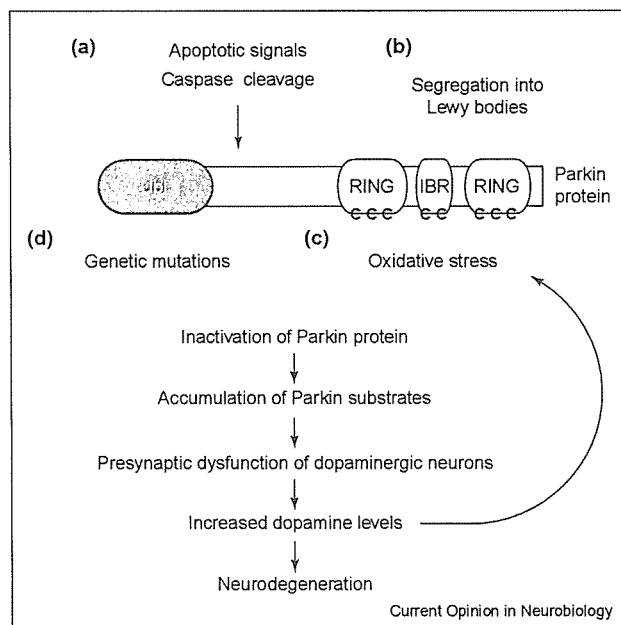
that its over-expression and gene triplication can cause neurodegeneration, which suggests that α -synuclein might play a part in the pathogenesis of PD [3,4]. LBs are intracytoplasmic eosinophilic inclusions composed of a core of granular and filamentous material surrounded by radiating filaments 10–15 nm in diameter. They are frequently found in affected neurons, including those of the substantia nigra, in the brains of patients with typical PD. This strongly suggests that there is an abnormality of protein turnover in PD.

Autosomal recessive juvenile Parkinsonism (AR-JP) is the most frequent form of familial PD. Mutations in the *parkin* gene were originally discovered from the linkage study of Japanese AR-JP families in 1998 [5]. Thereafter its mutations have been found worldwide. In patients with AR-JP, loss of dopaminergic neurons and consequently parkinsonian symptoms mostly occur without LB formation [6]. It has been demonstrated that wild type Parkin has ubiquitin ligase (E3) activity and that AR-JP-related mutant Parkin proteins do not [7–9]. Here, we discuss the recent studies on the physiological and pathophysiological role of Parkin.

Parkin as a ubiquitin ligase and its co-factors

Parkin has a ubiquitin-like domain (Ubl) at its amino-terminus and two really interesting new gene (RING) fingers flanking a cysteine-rich domain, known as the in between RING fingers (IBR) region (Figure 1). Several studies have recently revealed that numerous proteins with RING finger motifs have ubiquitin-protein ligase activity, which functions by itself or forms a complex with other components. An F-box (the name was given from a conserved motif originally found in cyclin F) protein with WD (Trp-Asp) repeats, hSc1-10, and cullin-1 (one of cullin/CDC53 family members) have been shown to complex with Parkin, thus forming a SCF-like (named after their main components, Skp1, Cullin, and an F-box protein) E3 complex, which is involved in the degradation of cyclin E [10]. The authors of this report have suggested that, under normal circumstances, Parkin might regulate cyclin activity, and that neurodegeneration might occur in PD because of a disruption of this process. Parkin is also associated with the molecular chaperone heat shock protein 70 (Hsp 70), as well as another E3 carboxy-terminus of Hsc70-interacting protein (CHIP) [11,12]. CHIP, which was originally reported as an Hsc/Hsp70-binding protein, functions as a quality control monitor of proteins through its E3 function [13]. Recognition of abnormal proteins by Hsp70 and subsequent ubiquitination by CHIP support the regulation of quality control of intracellular proteins.

Figure 1



Proposed hypothesis of Parkin inactivation and subsequent neurodegeneration based on recent findings. The function of Parkin can be disturbed by four different factors. **(a)** Extracellular stress, inflammation, and insufficient neurotrophic factors can activate caspases that degrade Parkin [33,34]. **(b)** Protein inclusions, such as LBs, resulting from impairment of proteasome activity might sequester Parkin thereby eliminating its activity, although there is discrepancy among the results of immunostaining in LBs with different Parkin antibodies [17,30,31,39]. **(c)** Oxidative stress within dopaminergic neurons has been suspected to be involved in PD, as an accumulation of iron is frequently observed in areas of degeneration in PD. Reactive oxidants, as well as dopamine/dopa-quinones, might modify a cluster of cysteine residues (represented by 'C') responsible for the E3 activity of Parkin, thus resulting in the precipitation of Parkin [22*,23]. Increased levels of intracellular dopamine and dopamine metabolites due to inactivation of Parkin might further perpetuate adduct formation with the cysteine residues of Parkin [42**,43*]. **(d)** Genetic mutations of the *parkin* gene, among other factors, might disturb Parkin function, resulting in an accumulation of Parkin substrates and subsequent neurodegeneration. The substrates of mammalian Parkin might differ from those of fly Parkin, such that a deficiency of Parkin might have different effects in the two species [25*].

As Parkin also ubiquitinates polyglutamine proteins through an Hsp70-mediated interaction, it is possible that Parkin functions in the same way as CHIP in degrading certain aberrant proteins through E3 activity after binding to Hsp70 [12]. In addition, CHIP cooperates with Parkin in the ubiquitination reaction responsible for endoplasmic reticulum-associated degradation (ERAD) [11].

Parkin substrates

There are a growing number of studies that report the identity of proteins that are ubiquitinated by Parkin (Table 1). Here, we feature four proteins out of Parkin's putative substrates. Cell division control-related protein

1 (CDCrel-1), which belongs to the Septin GTPase family, was the first reported Parkin substrate [9]. Although CDCrel-1 is thought to regulate neurotransmitter exocytosis, central nervous system abnormalities have not been detected in CDCrel-1-deficient mice. Specifically, alterations in synaptic firing have not been observed [14]. By contrast, over-expression of CDCrel-1 delivered by a viral vector induces dopamine-dependent neurodegeneration in the rodent brain [15*]. Another putative substrate of Parkin, the Pael receptor (Pael-R), which is a G protein-coupled orphan receptor, is abundantly expressed in dopaminergic neurons in the substantia nigra and tends to unfold even in a physiological condition. Thus, there is a possibility that excessive levels of unfolded Pael-R might lead to neuronal death as a result of unfolded protein stress. When Pael-R was expressed in all the neurons of the brain in *Drosophila melanogaster*, selective neurodegeneration of dopaminergic neurons was observed over time [16*]. Recently, immunolocalisation techniques have revealed Pael-R presence in Lewy bodies [17]. The p38 subunit of the aminoacyl-tRNA synthetase (ARS) complex is also ubiquitinated by Parkin [18]. The p38 subunit has been identified with immunolabelling in LBs in idiopathic cases of PD, whereas the ARS complex including the p38 subunit has been associated with protein biogenesis in a number of tissues as well as the brain [18]. It is believed that Synaptotagmin XI is localized with the secretory granules of neurotransmitters and plays a part in exocytosis stimulated by calcium ions. Synaptotagmin XI, which has been immunolabelled in LBs as well as normal neurons in the substantia nigra, is ubiquitinated and degraded in a Parkin-dependent manner [19]. Parkin inactivation causes a failure of Synaptotagmin XI to be ubiquitinated, and it is possible that this accounts for the disorder of dopamine release that is seen in Parkin-deficient mice.

Parkin and α -synuclein

A number of investigators in this field question whether or not there is a relationship between *parkin* and α -synuclein, as mutations of both these genes are causative of familial PD. Some studies have shown Parkin to attenuate wild type or mutant α -synuclein-mediated neurotoxicity within tyrosine hydroxylase (TH)-positive neurons, however, Parkin has not been observed to ubiquitinate α -synuclein *in vitro*. When mutant α -synuclein escapes the regulation of quality control of intracellular proteins, it sensitizes catecholaminergic neurons and impairs proteasomal activity [20]. Over-expression of Parkin rescues TH-positive cells from mutant α -synuclein toxicity and the effects of proteasomal inhibition [20,21]. Similar results have been observed in TH-positive *Drosophila* neurons [16*]. Now that Parkin-deficient mice can be used as a model, the genetic link between these two genes, as well as other genes involved in familial cases of PD, can be investigated in mammals.

Table 1

Reported substrates of Parkin.				
Protein	Physiological or pathological function	Immunopositivity detected in LBs	Methods of identification	References
CDCrel-1	Septin family protein with unknown function	–	Y	[9,44]
O-glycosylated α -synuclein	Isoform of α -synuclein with unknown function	N.D.	I	[45]
Pael receptor	Orphan G-protein coupled receptor	+	Y	[17,46]
p38 subunit of the aminoacyl-tRNA synthetase	Role in protein biosynthesis	+	Y	[18]
Synaptotagmin XI	Regulates exocytosis of neurotransmitters	+	Y	[19]
Expanded polyglutamine(polyQ) proteins	Aberrant proteins responsible for polyQ diseases	N.D.	I	[12]
α/β -tubulins	Microtubule proteins	+	I	[47,48]
Synphilin-1	α -synuclein-binding protein	+	I	[49,50]
Cyclin E	Cell cycle regulation of mitotic cells; unknown function in neurons	N.D.	I	[10]
SEPT5_v2/CDCrel-2	SEPT5_v2 is highly homologous with CDCrel-1	N.D.	Y	[51]

Common features or binding motifs have not been identified among these reported substrates of Parkin. Some of them have been observed within LBs or Lewy neuritis ('+' and '–' mean immunopositive and immunonegative, respectively, 'N.D.' indicates not determined).

This finding suggests that Parkin dysfunction might be involved in some part of PD as well as AR-JP. 'Y' and 'I' in methods of identification indicate yeast two-hybrid screening and immunoprecipitation (or pull-down)/western blot assay, respectively.

The role of Parkin against stress

Oxidative stress is thought to play a part in neurodegeneration. As the cysteine residues of Parkin are integral to its E3 activity, alteration of these residues by reactive materials, such as an oxygen radical, might impair the function of Parkin. Indeed, peroxide has been shown to generate mis-folded Parkin [22^o]. In addition, the three amino acids at the carboxy-terminal of Parkin are necessary for proper folding and probably its function, such that a pathogenic mutant, known as W453Stop, fails to adopt the native conformation of Parkin. Interestingly, induction of chaperones by heat shock reduces the mis-folding of Parkin that occurs following treatment with peroxide. One Parkin-binding protein, Hsp70, along with its co-chaperone, Hsp40, has been observed to inhibit partially the precipitation of both peroxide-treated and mutant Parkin *in vitro*, although recovery of Parkin's E3 activity has not been observed. The results of another study suggest that impairment of proteasomal activity by stable expression of Parkin mutants leads to accumulation of damaged proteins and lipids due to oxidation, thus sensitizing neurons to various forms of stress, which results in neuronal death [23].

Over-expression of Parkin has been observed to attenuate C2-ceramide-mediated mitochondrial swelling prior to cell death [24]. Subcellular fractionation experiments have revealed substantial amounts of Parkin on the outer mitochondrial membrane, however, the mechanism by which over-expression of Parkin might protect mitochondrial integrity is unknown as yet. The only orthologous gene of human *parkin* has been discovered in the *Drosophila* genome. This gene product has 59% overall similarity with human Parkin. Notably, *Drosophila parkin* null mutants have been found to exhibit markedly different pathology than that observed in human cases of PD [25^o].

Specifically, evidence of degeneration of TH-positive neurons in the brains of *Drosophila parkin* null mutants is lacking. The mechanisms behind the remarkable phenotypic differences between Parkin deficient humans and flies are still unknown, although there is a possibility that the *Drosophila* ortholog recognizes a fly-specific substrate(s), which is not associated with AR-JP. Importantly, it has been observed that mitochondrial dysfunction in some muscles and spermatids that undergo high energy metabolism can be reversed upon transgenic expression of *Drosophila* Parkin. These findings indicate that Parkin might maintain mitochondrial function even in humans, thereby protecting cells from the oxidative stress that is generated by mitochondrial dysfunction.

Ubl-containing proteins, such as Rad23 and Dsk2, interact with the 26S proteasome through the Ubl, thus linking the 26S proteasome to ubiquitination enzymes. The Ubl of Parkin has a typical ubiquitin fold and binds to Rpn10, Rnt6 and C3, all of which are subunits of proteasome complexes [12,26^o,27,28]. In addition, binding between Parkin and various proteasome complexes appears to be ATP-dependent [11]. The results of another study suggest that the Ubl might function as an unstable tag for breakdown despite the lack of necessity for Parkin auto-ubiquitination, thereby regulating the level of cellular Parkin [29]. Mutations affecting Ubl function have been identified in both humans (R42P) and *Drosophila* (A46T) with neurodegeneration in human and mitochondrial dysfunction in *Drosophila*, thus indicating the importance of the Ubl domain for Parkin function. A number of investigators have frequently observed processing of Parkin around the end of its Ubl domain [10,20,22^o,30–32]. Some of the enzymes involved in this processing were shown to be caspases, which suggests that apoptotic signaling following various forms of cell stress inactivates the

Parkin protein [33,34]. This idea is supported by the finding of an absence of Parkin following cerebral injury due to transient ischemia, and a subsequent reduction in ATP levels [35]. Although several lines of evidence suggest that up-regulation of Parkin enhances its protective function against unfolded protein stress, inconsistent observations imply the involvement of cell-type specific factors in the regulation of the *parkin* gene [7,35,36]. Astrocytes, which express lower levels of Parkin than hippocampal neurons, have a propensity to induce Parkin expression and subcellular redistribution of Parkin during unfolded protein stress, whereas hippocampal neurons do not [37]. This observation might partially explain why dopaminergic neurons as well as other neurons are especially vulnerable to any stress caused by generation of unfolded proteins.

Parkin in cellular protein inclusions and Lewy bodies

LBs are a pathological hallmark of PD. The presence of LBs in affected regions, among others, in PD indicates that improper handling of proteins might be involved pathogenesis of the disease. However, the mechanism by which LBs are formed and their role in neurodegeneration remain unknown. Neurodegeneration in AR-JP is not accompanied by obvious LB formation. By contrast, it has been demonstrated that both isolated LBs and LBs in paraffin sections are immunopositive for Parkin [17,31]. Protein inclusions, such as aggresomes, can be experimentally induced by proteasomal inhibition in both neuronal and non-neuronal cells. Considerable immunocytochemical analyses have reported that Parkin, as well as a number of other proteins within LBs, is localized in the cellular inclusions following exposure of cells to proteasome inhibitors [32,38,39,40,41]. This suggests that LBs and other cellular protein inclusions could work to isolate Parkin, thereby eliminating its function. This idea raises the possibility that sequestering of Parkin is a factor contributing to neurodegeneration even in idiopathic PD with LBs. By contrast, a series of immunohistochemical experiments using different monoclonal and polyclonal antibodies to Parkin failed to detect Parkin-immunoreactivity in LBs [19,30]. Another immunocytochemical study has reported that endogenous Parkin in human dopaminergic neuroblastoma SH-SY5Y cells is recruited into perinuclear inclusions after treatment with dopamine and a pro-apoptotic reagent staurosporine, as well as a proteasome inhibitor [32]. Although transgenic over-expression of Parkin suppresses cellular inclusions induced by these kinds of stress, the inhibition of inclusion formation by Parkin is not always associated with protection from cell death [32].

Animal models of AR-JP

The first reports of experiments conducted with Parkin-deficient mice come from two different research groups [42*,43*]. Although a macroscopic loss of nigrostriatal

dopaminergic neurons has not been reported, evidence of pre-synaptic dysfunction of dopaminergic and glutamatergic neurons has been found in association with altered behavior that could be caused by neuronal dysfunctions. Remarkably, it has been observed that Parkin-deficient mice have increased levels of dopamine and dopamine metabolites within their striatum. These phenomena suggest that Parkin is necessary for maintenance of the synaptic functions in dopaminergic neurons as well as other neurons.

Conclusions

The ubiquitin system plays a part in the sorting of membrane proteins, endocytosis of receptors at the plasma membrane, transactivation of genes, and protein degradation. However, several lines of evidence suggest that Parkin takes a role in protein degradation through binding of its Ubl to the proteasomes. The recent development of Parkin-deficient mice will help to confirm whether or not accumulation of proposed substrates of Parkin is responsible for neurodegeneration, as well as to assist in the identification of novel substrates, thus shedding light on the pathogenesis of AR-JP (Figure 1). For example, by crossbreeding mice it will be possible to analyse genetic interactions of Parkin and its substrates with the hope of finding a true substrate responsible for AR-JP, which will be the first step to the next generation of PD study.

Acknowledgements

Work in our laboratory was partially supported by the Ministry of education, Science, Sports and Culture, Grant-in-Aid for Scientific research on Priority areas, Advanced Brain Science Project #15016120 and Scientific Research (A) #14207032 to R Takahashi. Young Scientists (A) #15680011 and a grant from Special Postdoctoral Researcher of RIKEN to Y Imai.

References and recommended reading

Papers of particular interest, published within the annual period of review, have been highlighted as:

- of special interest
 - of outstanding interest
1. Polymeropoulos MH, Lavedan C, Leroy E, Ide SE, Dehejia A, Dutra A, Pike B, Root H, Rubenstein J, Boyer R *et al.*: **Mutation in the alpha-synuclein gene identified in families with Parkinson's disease.** *Science* 1997, **276**:2045-2047.
 2. Krüger R, Kuhn W, Müller T, Woitalla D, Graeber M, Kosel S, Przuntek H, Epplen JT, Schols L, Riess O: **Ala30Pro mutation in the gene encoding alpha-synuclein in Parkinson's disease.** *Nat Genet* 1998, **18**:106-108.
 3. Trojanowski JQ, Goedert M, Iwatsubo T, Lee VM: **Fatal attractions: abnormal protein aggregation and neuron death in Parkinson's disease and Lewy body dementia.** *Cell Death Differ* 1998, **5**:832-837.
 4. Singleton AB, Farrer M, Johnson J, Singleton A, Hague S, Kachergus J, Hulihan M, Peuralinna T, Dutra A, Nussbaum R *et al.*: **Alpha-synuclein locus triplication causes Parkinson's disease.** *Science* 2003, **302**:841.
 5. Kitada T, Asakawa S, Hattori N, Matsumine H, Yamamura Y, Minoshima S, Yokochi M, Mizuno Y, Shimizu N: **Mutations in the parkin gene cause autosomal recessive juvenile parkinsonism.** *Nature* 1998, **392**:605-608.
 6. Mizuno Y, Hattori N, Matsumine H: **Neurochemical and neurogenetic correlates of Parkinson's disease.** *J Neurochem* 1998, **71**:893-902.